DEFORMATION MONITORING USING INSAR AND ARTIFICIAL REFLECTORS

Ivana, HLAVÁČOVÁ[1], Lena, HALOUNOVÁ[1], Květoslava, SVOBODOVÁ[1]

[1]Department of Mapping and Cartography, Faculty of Civil Engineering, Czech Technical University, Thákurova 7, 166 21, Prague, Czech republic

ivana.hlavacova@fsv.cvut.cz, lena.halounova@fsv.cvut.cz, kvetoslava.svobodova@fsv.cvut.cz

Abstract

The SAR interferometry (InSAR) method can be used to create digital elevation model (DEM), or to monitor terrain deformation or some features of the atmosphere. The method uses several satellite radar images, to form interferograms from pairs of them. The interferogram always contains several components: the flat Earth, topography, deformations, atmospheric influence and noise. The aim is typically to extract one of the components and therefore, it is possible to estimate and subtract (or neglect) the others.

A big problem of this method is so-called decorrelation, i.e. if the noise is significantly higher than other components. Mostly, it happens in vegetated areas - forests, agricultural fields, meadows, mostly during late spring, summer and early autumn. Such vegetated areas can be monitored only during winter (if no snow is laying), but with lower accuracy. Much better results can be gained in urban areas, which are stable in time (in the order of centimetres). The decorrelation can be also found if there is a long time or long distance between the acquisitions of the scenes in a pair.

We deal with monitoring of deformations, which occur due to undermining or subsidence (on waste dumps), or due to landslides, mostly in the Nothern-Bohemian coal basin. We cooperate with the Coal Services, a.s., company, and within this project there were 11 artificial corner reflectors installed in the mines surroundings (near the Most city). The places to install the reflectors were selected by the company as the most important places to monitor. This is the only way to monitor areas containing a very small amount of artificial objects.

Now, the corner reflectors are monitored by German satellite TerraSAR-X, which enables acquisition of images with resolution of approx. 3x3 m. The corner reflectors can be found in the scene as very light points (with respect to their surroundings), about 2x2 pixels large. It is impossible to find one of the reflectors, because it is placed in the area of radar foreshortening/layover. The period of this satellite is 11 days, the acquisition is performed (due to financial reasons and with respect to the deformation rate) once in 33 days.

The basic interferometric processing of 4 available scenes was performed, both for the whole area and the corner reflectors alone.

Keywords: Synthetic aperture radar, interferometry, subsidence, Northern Bohemian coal basin, artificial corner reflectors

INTRODUCTION, AREA AND PROJECT DESCRIPTION

The Northern-Bohemian coal basin is full of brown coal. Both in history and today, it is being exploited. In history, the most frequent way was deep-mining, with the risk of subsidence of undermined areas. Today, there are many huge open-pit mines and waste dumps, with a similar risk of subsidence - however, reclamation was mostly performed in a way in order to minimize the impact of the subsidence - most of the area is forested, there can also be found water surfaces, horse racing grounds, and only rarely, when there is no other possibility, a road, railway etc. is built on a waste dump. New family houses are being built on old waste dumps.

In cooperation with Czech Coal, a.s. company, there were 11 artificial corner reflectors installed in the area. Their list can be found in table 1. Last spring, the reflectors started to be monitored by the TERRASAR-X satellite. List of available data due to date of paper submission can be found in table 2.

The TERRASAR-X [1] satellite is a German satellite, with a SAR on-board. Its period of overpass is only 11 days, and the wavelength is only 3.1 cm (X-band). Due to the fact that fast deformations are not expected in the area of interest (in built-up areas which can be monitored), we decided to order one scene in 33 days. The incidence angle for these scenes is about 30°. The scenes were acquired in the StripMap mode with resolution of about 3x3 metres.

Table 1. Corner reflectors, placed in the area of interest. Point 9, at the dam near the Vysoká Pec village, is invisible in the scene due to the radar shadow (scenes are from descending pass). The intensity is only approximate and is computed as a mean for all scenes.

Point	Name	Y	X	range	az.	intensity
1	ČSA	797910.59	986137.97	1568	2700	6×10^7
2	ČSA lom	798828.08	984351.49	2474	2030	5×10^6
3	Centrum	793904.55	982765.86	49	509	5×10^6
4	Horní Jiřetín	796600.26	980927.46	1842	103	2×10^6
5	Černice	798208.87	981182.20	2666	479	2×10^6
6	monitoring	799860.73	982529.26	3266	1362	7×10^7
7	Jezeří	800040.38	982355.30	3310	1312	3×10^6
8	ČS - ČSA	801088.68	983470.47	3754	1991	1×10^6
9	přehrada u Vys. Pece	802050.76	982886.82	invisible (shadow)		
10	Vysoká Pec ob. úřad	802976.67	985356.52	4387	3159	4×10^6
11	mont. místo Vrskmaň	801578.94	988818.49	2989	4518	5×10^6

Table 2. List of available scenes. All scenes are acquired in descending mode, at approx. 5:25 UTC.

Date	Temp. baseline [days]	Perp. baseline [m]
2011-06-17 (master)	*0*	*0*
2011-07-20	33	-145
2011-08-22	66	3.5
2011-09-24	99	-143

An artificial reflector is expected to be found in the scene as a very high-intensity point, in comparison to its surroundings. It is advised that the reflectors are not installed close to object which can also have high reflectivity (buildings, bridges over roads or rivers).

All points were found in all the scenes, except for point 9, which is, unfortunately, situated in radar shadow. In most cases, the reflectors are visible as a light square (mostly 2x2 points), in some cases it is a cross, in some cases there are also other light pixels.

Using intensity, the position of the reflectors were estimated with a sub-pixel accuracy, and also the intensity was interpolated for such an estimated position. The estimation is performed in the GAMMA software [2]. In table 1, the intensity is given only approximately in order to allow comparison among individual reflectors. Comparing the estimated reflector positions, standard deviation for each point is 0.1 pixel at maximum (for both range and azimuth coordinates).

We tried both types of processing, to estimate Earth surface deformations either only for the reflectors, or for the whole scene crop, and present preliminary results (we are still waiting for more scenes to be acquired) of both types.

PROCESSING OF THE WHOLE SCENE CROP

The four scenes acquired were co-registered to a selected master (the first acquisition), and then cropped. Six interferograms were formed of them. The interferograms are mostly decorrelated due to vegetation, but artificial objects, such as buildings, roads, bridges, railway etc. can be well recognized.

For topography subtraction, we use the SRTM (Shuttle Radar Topography Mission) DEM (digital elevation model), acquired in 2000 using X-band antenna [3]. Because SRTM was primarily designed for C-band, the X-band data contain "holes", places which were not mapped due to shorter swath. In our case, this is the case of the bottom-left corner; fortunately, there is no corner reflector placed in this area.

The SRTM X-band DEM is classified as precise (however, it is 11 years old, so not very up-to-date in open-pit mines). However, the resolution of the scenes is so good that in some cases, we can see a phase gradient over a wall of a building - and this cannot be covered in the DEM with resolution of 1" (about 20-30 m for our latitude).

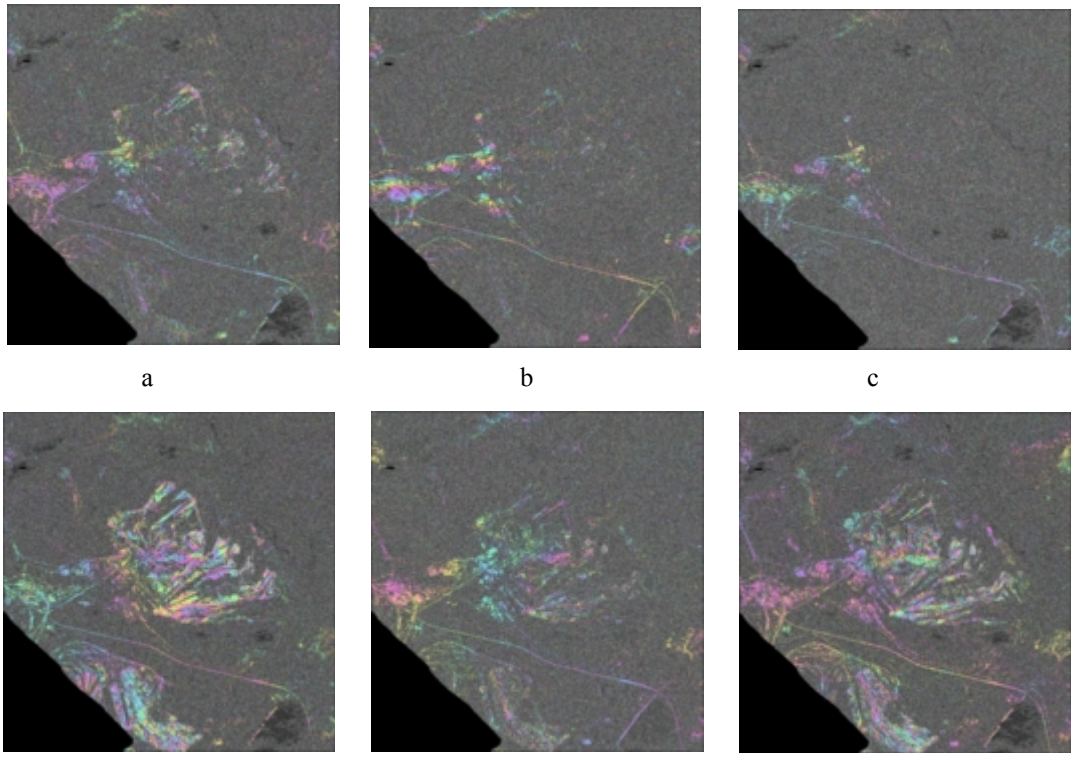

Fig. 1. Interferogram phase maps, the colorsale is displayed in figure 2 and corresponds to 2π. Created from scenes acquired (a) 11-06-17 and 11-07-20, (b) 11-06-17 and 11-08-22, (c) 11-06-17 and 11-09-24, (d) 11-07-20 and 11-08-22, (e) 11-07-20 and 11-09-24, (f) 11-08-22 and 11-09-24. Interferograms (b) and (e) are of very short perpendicular baseline, i.e. no DEM error is expected. However, interferogram (b) contains visible fringes (in the azimuth direction), which can be attributed only to atmoshperic delay or orbit errors. Within the open mines (coherent only in (d), (e), (f)), fringes are expected due to the out-of-date DEM. The line between the open mines is the Ervěnice corridor - railway, road and pipeline built on a waste dump in 1980s (the coherent line is the railway). The line approx. perpendicular to the Ervěnice corridor in its lower part is the Kyjická dam. The built-up area on the left part of the scene is Komořany.

Fig. 2. Colorscale used for the interferogram and deformation maps.

Among the six interferograms, we can find two with a very short perpendicular baseline (shorter than 5 m) - both with temporal baseline of 66 days. In the interferograms with the perpendicular baseline of about 145 m, only 1 m error in the DEM causes a phase error of about 11 degrees.

However, as an additional error source, besides the DEM error, we must consider the atmospheric delay variation. This is expected to be of a long wavelength, i.e. should cause phase differences on long distances; and therefore short distance phase differences are to be considered deformations.

In all interferograms in figure 1, one can see phase trends. In interferogram (b), the fringes are probably caused by atmospheric delay variation, however, if this was the case, we should see it also in some other interferograms. The same applies for an orbit error. A small DEM error is expected in this case due to the very short perpendicular baseline.

Interferograms (a), (c), (d) and (e) present a slow trend (let us neglect the colour variations of the open mines, where there is certainly up-to-date DEM). This trend can be probably attributed to atmospheric delay variations. In interferograms (c) and (e), one can find a phase (colour) change at the beginning of the corridor itself (at the double bend). This was not investigated yet, and we plan to prepare a mask (to mask out the open pit mines) and estimate the atmospheric delay as the trend.

We also tried the IPTA (Interferometric Point Target Analysis) processing. IPTA is implemented in the GAMMA software [2] and is similar to other (better-documented) methods of Permanent Scatterers [4] or Persistent Scatterers [5]. However, the recommended number of scenes for this method is at least 10. For a small number of scenes, it is more difficult to select the points to be processed , and also estimate a suitable threshold for a posteriori standard deviation. In addition, during the adjustment, phase ambiguities are estimated, and there are many more possibilities to estimate them with just a small change of the resulting standard deviation (due to the small number of inputs).

A priori point selection is performed on the basis of MSR (mean-to-sigma-ratio), described in [5]. Both mean and standard deviation (sigma) are computed from the intensity information of each pixel (from all scenes available). However, such a measure becomes statistically more precise for a higher number of scenes. Software GAMMA [1], however, during the evaluation also takes into account the intensity of the neighbouring points, and therefore only pixels that are much brighter than their surroundings are really selected. On the other hand, allows to perform the selection on a different basis, based only on the surroundings of each pixel (for each scene separately), but according to our older tests, better results were achieved using the statistical method even for small number of scenes.

After processing, i.e. the adjustment with the ambiguity estimation, a posteriori point selection is performed, on the basis of the a posteriori standard deviation. The threshold recommended in the GAMMA software does not work here, it gives too many points with irrelevant results, and even if lowering the threshold helps, the resulting deformation map (see fig. 3) still contains many points which do not seem to be appropriate. This problem is expected to be improved with a higher number of scenes to be acquired in the future.

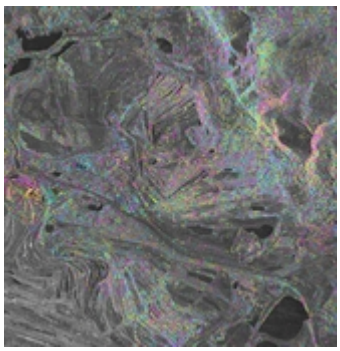

Fig. 3. Deformation map from the IPTA method. The colorscale is displayed in figure 2 and corresponds to and corresponds to 50 cm/year.

PROCESSING OF THE REFLECTOR INFORMATION ALONE

In this case, after finding the reflectors, it is necessary to estimate their precise (sub-pixel) positions and interpolate the phase to this precise position. Software GAMMA implements two ways of doing that:

- the *ptarg* script, suitable to be used on original SLC (single-look complex) data (containing intensity and phase, but not yet paired and processed into interferograms)
- the *xpt_slc* script, which is part of the IPTA package. To be able to use it, one first need to make the point selection and then work only with the selected points.

The *ptarg* script

In our project, we are interested in the interferogram phase of the reflectors; however, we do not need the phase information of the original SLC data. Interferogram phase is the difference between phases of two scenes; however, with some adjustments: flat-Earth phase subtraction and DEM subtraction. The phase should not be filtered spatially, and we are not sure if spectral filtering is recommended (however; due to short baselines and zero Doppler centroid, filtering is expected to be almost useless).

Interferogram creation, flat-Earth and DEM subtraction is performed within the GAMMA software and we tried to apply the *ptarg* script on the result. However, the resulting interferogram contains only the phase component, with the intensity equal to 1 for all points. In this case, it is impossible to estimate the sub-pixel position of the reflector, because for the estimation, the intensity information is used. We therefore multiplied all interferograms with the intensity of the master scene (acquired on 2011-06-17) in order to estimate the precise position of the reflectors and its phase. The estimated intensity (approximate) can be found in table 1.

Using *ptarg*, we estimated the reflector positions and phase for all six interferograms (displayed in figure 1) and for all reflectors (except for reflector 9, which cannot be found in the image due to the radar shade). In all cases, the *ptarg* script was successful, the sub-pixel position was estimated and the phase interpolated. The *ptarg* script computes two values of interpolated phase: *peak phase* and *peak phase with phase gradients*. We did not know which one is better to use in this case, and tried to use both.

The estimated positions for each reflector differ by 0.02 pixel at maximum, which seems to be appropriate. To check the phase accuracy, we compute triangular sums: we select three scenes, make three interferograms containing only these scenes, and the phase sum of all of them is expected be 0 (except for noise, orbit errors and position estimate and interpolation errors).

However, this is not always the case. The triangular sums can be found in table 3.

Table 3. Triangular sums for the *ptarg* outputs (in radians), reduced for integer multiples of 2π. The triangle is constructed from the three interferograms created from the three scenes disclosed in the first column. For all points, numbered 1 to 11 (except for 9, which is invisible), the sum of estimated peak phases and sub of estimated “peak phases with phase gradients” is computed. It can be seen that only for the last triangle the “peak phase with phase gradients” is approximately constant for all points, however not close to zero. Unfortunately, this is not the case of previous triangles, but this problem can be solved only with more scenes.

The triangular sums, disclosed in table 3, seem to be random. Only in the case of the last row, these sums are approximately constant. This could mean that it is more suitable to use “peak phase with phase gradients” for the following processing; however, it is not evident why this does not apply to the previous three triangles. We hope that this will be more clear in future, with more available scenes.

Phases with such high (and random) triangular sums are useless to be processed.

Triangle		1	2	3	4	5	6	7	8	10	11
110617-	peak phase	-1.33	-2.60	-1.59	2.00	1.35	-2.84	-2.92	0.81	3.00	1.60
110720-	with ph. gr.	-1.23	-1.98	-2.51	-2.21	1.61	-2.46	-2.88	0.26	-3.00	0.15
110822											
110617-	peak phase	-0.12	0.55	3.06	1.96	0.79	-1.75	-1.21	2.97	0.19	-3.07
110720-	with ph. gr.	-0.10	0.61	3.08	1.14	0.82	-1.77	-1.37	2.66	-0.86	0.35
110924											
110617-	peak phase	0.30	1.87	-0.72	-2.88	-1.87	-0.13	0.78	2.12	1.99	1.35
110822-	with ph. gr.	-0.03	1.38	-1.85	2.09	-2.04	-0.72	0.34	0.98	0.85	-1.03
110924											
110720-	peak phase	-0.91	-1.28	0.92	-2.83	-1.31	-1.22	-0.93	-0.03	-1.48	-0.25
110822-	with ph. gr.	-1.16	-1.21	-1.15	-1.27	-1.25	-1.41	-1.17	-1.43	-1.30	-1.23
110924											

The *xpt_slc* script

The *xpt_slc* script is a part of the IPTA package, and – similarly to *ptarg* – estimates the position of the reflectors (point scatterers) with a sub-pixel accuracy. And although it also works for original SLC data, the resulting format is compatible with the following processing - interferogram creation, flat-Earth and DEM phase subtraction (both are estimated on the basis of the precise position). That means, that the results are expected to be more accurate than that of *ptarg*, and also that triangular sums should be close to zero or at least close to constant for all reflectors.

However, in the case of *xpt_slc*, not all reflectors were successfully identified as point scatterers in all scenes (reflectors 6 and 7 are missing in only one scene, but the others even in more of them). Reflector 11 was even not selected for processing in the a priori point selection, described above.

However it may seem that both scripts have the same basis, it is no way to override the inability of the *xpt_slc* script to detect some reflectors as point scatterers. This is the case of the reflectors with the lowest intensity (see table 1). Also, however the differences among the estimated positions of each reflector were usually less than 0.2 pixels for ptarg, for xpt_slc are the differences almost 1 pixel, which is probably the reason why some scenes are missing for a reflector.

Research in the near future will be devoted to comparison of the phase and intensity values between both scripts, in order to use the values estimated by *ptarg* for the subsequent processing.

CONCLUSIONS

There are still too few scenes in order to present any reasonable results. However, there are some notes about what the further processing may give:

- Individual reflectors can be well found in the images, except for reflector 9, which is situated in radar shadow. Reflectors 1, 2, 3, 10 are in all available scenes detected as point scatterers, reflectors 6 and 7 are missing only in one scene. The other reflectors may be inaccurately oriented or surrounded by other well-reflecting objects. Reflector 11 was even not selected as a point for IPTA processing.
- The *ptarg* script does not give satisfactory results. The source of inaccuracy may be the fact that the interferogram phase is then manually multiplied by image intensity (of the same image for all interferograms), but the phase reductions (flat-Earth and DEM phase) are computed not for the reflector position, but for the cell centre.
- More hopeful is the *xpt_slc* script. However, it does not detect all points as point scatterers, and also the variations in the estimated position is higher.

- Conventional interferometric processing gives reasonable results, there are scene pairs with very short perpendicular baselines; however, the interferograms made from such a pair are not as unicolour as expected, probably due to DEM errors (the resolution of the scene is much higher than the resolution of the available DEM).
- IPTA processing is not very promising yet; however, we still hope that this will improve with a higher amount of scenes available.

REFERENCES

[1] Infoterra, http://www.infoterra.de/terrasar-x-satellite, Oct 31, 2011.

[2] Gamma Remote Sensing, http://www.gamma-rs.ch, Oct 31, 2011.

[3] Deutsches Zentrum für Luft- und Raumfahrt, centaurus.caf.dlr.de:8080/eoweb-ng/licenseAgreements/

DLR_SRTM_Readme.pdf, Oct 31, 2011.

[4] Kampes, B (2006) Radar Interferometry: Persistent Scatterer Technique. Springer, Dordrecht, the Netherlands.

[5] Ferreti, A., Prati, C., Rocca, F. (2001) Permanent Scatterers in SAR Interferometry. IEEE Transaction on Geoscience and Remote Sensing, 39, 8-20.